PCCP

Accepted Manuscript

ROYAL SOCIETY OF CHEMISTRY

www.rsc.org/pccp

Chloride capping of $CdTiO_3$ for higher crystallinity and enhanced photocatalytic activity

Zameer Hussain Shah, Yuzhen Ge, Xijie Lin, Jinghai Xiu, Shufen Zhang, and Rongwen Lu*

State Key Laboratory of Fine Chemicals, Dalian University of Technology, Dalian 116024, People's Republic of China.

Author for Correspondence:

Rongwen Lu

State Key Laboratory of Fine Chemicals, Dalian University of Technology, Dalian 116024, People's Republic of China.

Fax: +86-411-84986292.

Tel: +86-411-84986270.

E-mail:lurw@dlut.edu.cn.

Abstract

The crystallinity of cadmium titanate ($CdTiO_3$) was greatly improved when synthesized at mild reaction conditions, in the presence of chloride. The highly crystalline $CdTiO_3$ showed much enhanced photodegradation of methyl orange (MO) under simulated sunlight. The $CdTiO_3$ was characterized by X-ray diffraction (XRD), transmission electron microscopy (TEM), X-ray photoelectron spectroscopy (XPS), N_2 adsorption/desorption, photoluminescence (PL), and UV/vis spectrometry. The enhanced photodegradation was attributed to the better charge separation owing to higher crystallinity.

Keywords: chloride capping, crystallinity, photodegradation, simulated sunlight.

Introduction

Semiconductor photocatalysis is significantly influenced by the extent of crystallization i.e. crystallinity.[1-5] Better charge separation and transfer of these photoexcited charges to the active sites are the main prerequisites to achieve higher photocatalytic activity.[6-10] The process of charge separation and transfer is dominated by the semiconductor crystal form.[11, 12] The relation between crystal form and photocatalysis has mainly been investigated in the context of dominant crystal-facets.[13, 14] Some recent studies have demonstrated that the higher crystallinity can also improve charge separation and transport by reducing surface defects resulting in the enhanced photocatalytic activity.[7, 15-17] The crystallinity of semiconductors is usually increased either by higher temperature or prolonged reaction time during the synthesis.[18] However, both these strategies lead to the grain growth and reduced

surface area which significantly lower the photocatalytic activity.[18-20] Hence, it is highly imperative to synthesize semiconductor nanoparticles at low temperature and short reaction time.

Here we anticipate to employ the microemulsion based synthesis in presence of a capping agent to address the above mentioned issues. Microemulsions are well known for the fabrication of small sized nanoparticles at low temperature and short processing time[21] while the capping agents can be used to achieve the desired crystallographic growth. [22-25] We selected cadmium titanate ($CdTiO_3$) as a model compound and chloride as a model capping agent. $CdTiO_3$ has been reported to show promising results for photocatalysis. De Anda Reyes et al. reported the synthesis and photocatalytic activity of CdO+$CdTiO_3$.[26] Similarly Pant et al. synthesized CdS/$CdTiO_3$ which showed photocatalytic activity for dye degradation and hydrogen release.[27] However, these studies showed that $CdTiO_3$ alone has no significant photocatalytic activity. Chloride is well known to strongly influence the crystallinity of cadmium chalcogenides.[28] Nonetheless, there have been no reports to study the effect of chloride on the other compounds of Cd e.g. CdO etc.

Now for the first time, we report the chloride assisted synthesis of $CdTiO_3$ with higher crystallinity and enhanced photocatalytic activity. $CdTiO_3$ synthesized in the presence of Cl^- showed better crystallinity and excellent photodegradation of methyl orange (MO) under simulated sunlight irradiation. On the other hand, $CdTiO_3$ synthesized in the absence of Cl^- lacked in crystallinity and showed very little photocatalytic activity.

Materials and methods

Materials

All chemicals were analytical grade and used without further purification. Polyoxyethylene (20) cetyl ether (Brij-58) was purchased from Acros. Tetrabutyl titanate (TBT), cadmium nitrate tetrahydrate ($Cd(NO_3)_2 \cdot 4H_2O$), cadmium chloride hemipentahydrate ($CdCl_2 \cdot 2.5H_2O$), ammonium hydroxide ($NH_3 \cdot H_2O$ 25%-28%), isopropyl alcohol (IPA), ethylene glycol (EG), sodium chloride (NaCl), Triethanolamine (TEA), t-butyl alcohol (TBA), *p*-benzoquinone (*p*-BQ), and methyl orange were all purchased from Sinopharm Chemical Reagent Co. Ltd. (SCRC). Deionized water (18.2MΩ) was used throughout the experiments.

Synthesis of $CdTiO_3$

In a typical synthesis, 6.738 g of Brij-58 was taken in a one-neck flask containing 30 mL cyclohexane. The temperature was kept at 50 °C throughout the synthesis. After stirring for 15 min, 1 mL of 0.25 M NaCl (EG) followed by 1 mL of 0.5 M $Cd(NO_3)_2 \cdot 4H_2O$ (EG) were added. After stirring for 20 min, 0.35 mL $NH_3 \cdot H_2O$ was added. Solution turned milky in the case of NaCl while it remained colorless when no NaCl was used (Fig. S1). After another 20 min, 0.4 mL, 0.2 mL, and 0.2 mL TBT was added successively having a gap of 15 min each. After 1 h of the last TBT addition, 30 mL IPA was added. Then the precipitate was separated by centrifugation followed by washing with IPA. The precipitate was dried overnight at 100°C and then calcined at 500°C for 2 h to obtain the powder. For comparison, pure TiO_2 was also prepared by the same method without the addition of NaCl and Cd precursor.

Characterization

Morphological studies were carried out by transmission electron microscopy (TEM). TEM analysis was carried out at room temperature on a JEOL JEM-2000 EX transmission electron microscope using an accelerating voltage of 120 kV. High resolution TEM images were obtained on a JEM-2100F (JEOL) transmission electron microscope operated at 200 kV. The XRD pattern was recorded on a Rigaku DMAX IIIVC X-ray diffractometer with Cu-Kα (0.1542 nm) radiation scanning from 10° to 80° (2θ) at the rate of 6°/min. XPS was acquired by VG ESCALAB 250 with an Al-Kα X-ray source operating at 150 W (15 kV). The binding energies were calibrated using the C 1s peak at 284.6 eV. The curve fitting was performed by XPS PEAK 4.1 software. UV/vis absorption spectra were obtained by JASCO UV-550. Photoluminescence (PL) spectra were recorded on a fluorescence spectrophotometer (Hitachi F 7000, Japan). The N_2 adsorption-desorption measurements were carried out on a Micrometrics ASAP 2010 surface area analyzer.

Photocatalytic degradation of methyl orange (MO)

The synthesized $CdTiO_3$ or TiO_2 (0.040 g) was added to a 50 mL MO solution (10 mg/L) in a beaker. The solution was stirred magnetically under dark for 30 min at 30 °C. The light source used was a Xe lamp (AULLT Cell-HFX300). Simulated sunlight light was irradiated on the solution and a 4 mL aliquot was taken at regular intervals of time. The photocatalytic activity was monitored by analyzing the aliquot samples on a UV-visible spectrophotometer (Agilent 8453) at 465 nm. Percent degradation (%D) of MO was calculated using the following equation:

$$\%D = (C_0-C)/C_0 * 100\%$$

Where C_0 is the concentration before irradiation and C is the concentration at any sampling time.

Results and Discussion

Synthesis and Characterization

$CdTiO_3$ was synthesized in a reverse microemulsion. The synthesis procedure is depicted in scheme 1. During the synthesis, NaCl played a very important role in determining the properties of the $CdTiO_3$. Ammonia solution was added to facilitate the hydrolysis of TBT. Addition of $NH_3 \cdot H_2O$ did not bring any apparent change in the solution when no NaCl was used. However, when $NH_3 \cdot H_2O$ was added in the presence of NaCl, the solution immediately turned milky (Fig. S1). It is assumed that this milky appearance was due to the formation of $Cd(NH_3)_4Cl_2$ which is insoluble in the reaction mixture. The solution remained milky throughout the rest of solution phase synthesis.

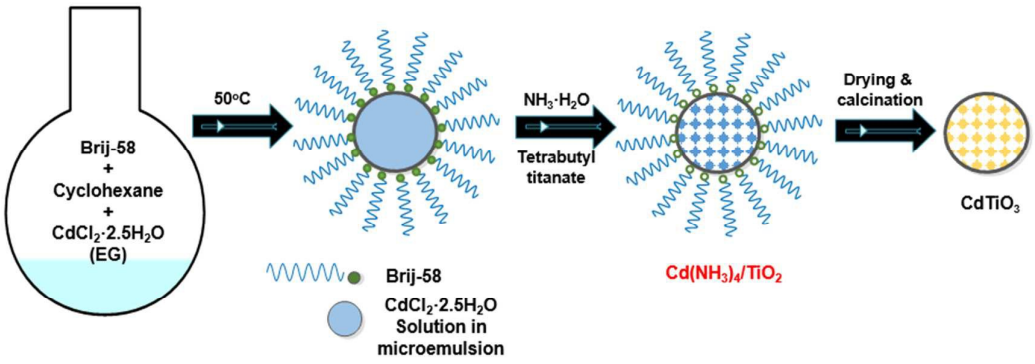

Scheme 1. Schematic representation of the synthesis of $CdTiO_3$.

After calcination, the $CdTiO_3$ were subjected to various analytical techniques for characterization. Fig. 1 shows the XRD patterns of the as synthesized powders. The XRD patterns show the presence of anatase along with $CdTiO_3$. A strong peak for

anatase (101) can be observed at 2θ=25.3° (JCPDS, no. 86-1157). No facets of high energy were observed when $CdTiO_3$ was synthesized in the absence of NaCl. However, at optimum NaCl concentration, a number of characteristic facets appeared in the XRD patterns. $CdTiO_3$ synthesized at optimum NaCl concentration was determined by its peaks at 2θ=17.9° (003), 2θ=20.4° (101), 2θ=22.9° (012), 2θ=31.1° (104), 2θ=34.1° (110), 2θ=50.7° (116), and 2θ=59.3° (214) (JCPDS, no. 29-0277). The presence of anatase along with $CdTiO_3$ has also been reported previously.[29]

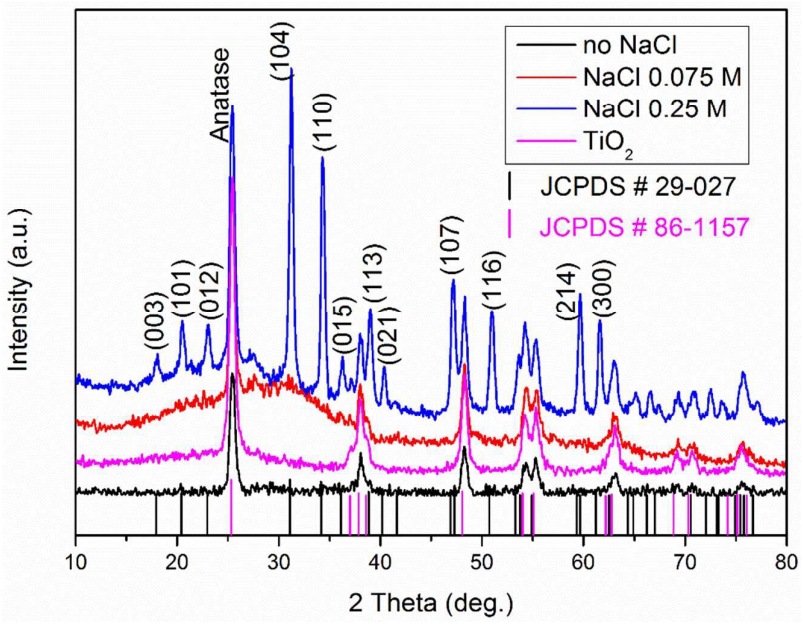

Fig. 1 XRD patterns for $CdTiO_3$ and as synthesized TiO_2.

$CdTiO_3$ has irregular morphology when synthesized in the absence of NaCl as shown in Fig. 2a. The addition of NaCl brought a dramatic effect on the morphology of $CdTiO_3$. Even a small amount i.e. 1 mL 0.075 M NaCl resulted in some sort of regular morphology (Fig. 2b). The morphology kept improving with the increase in NaCl concentration. Fig. 2c is the TEM for $CdTiO_3$ synthesized in the presence of 1 mL 0.25 M NaCl. The morphology at this concentration is a mixture of bars and cubes. A

further increase in NaCl concentration did not bring any considerable change to morphology, crystallinity, or photocatalytic activity, hence we assumed that 1 mL 0.25 M NaCl is the optimum concentration to achieve best results at our experimental conditions. HRTEM (Fig. 2d) confirmed that the $CdTiO_3$ synthesized in the presence of chloride was highly crystalline.

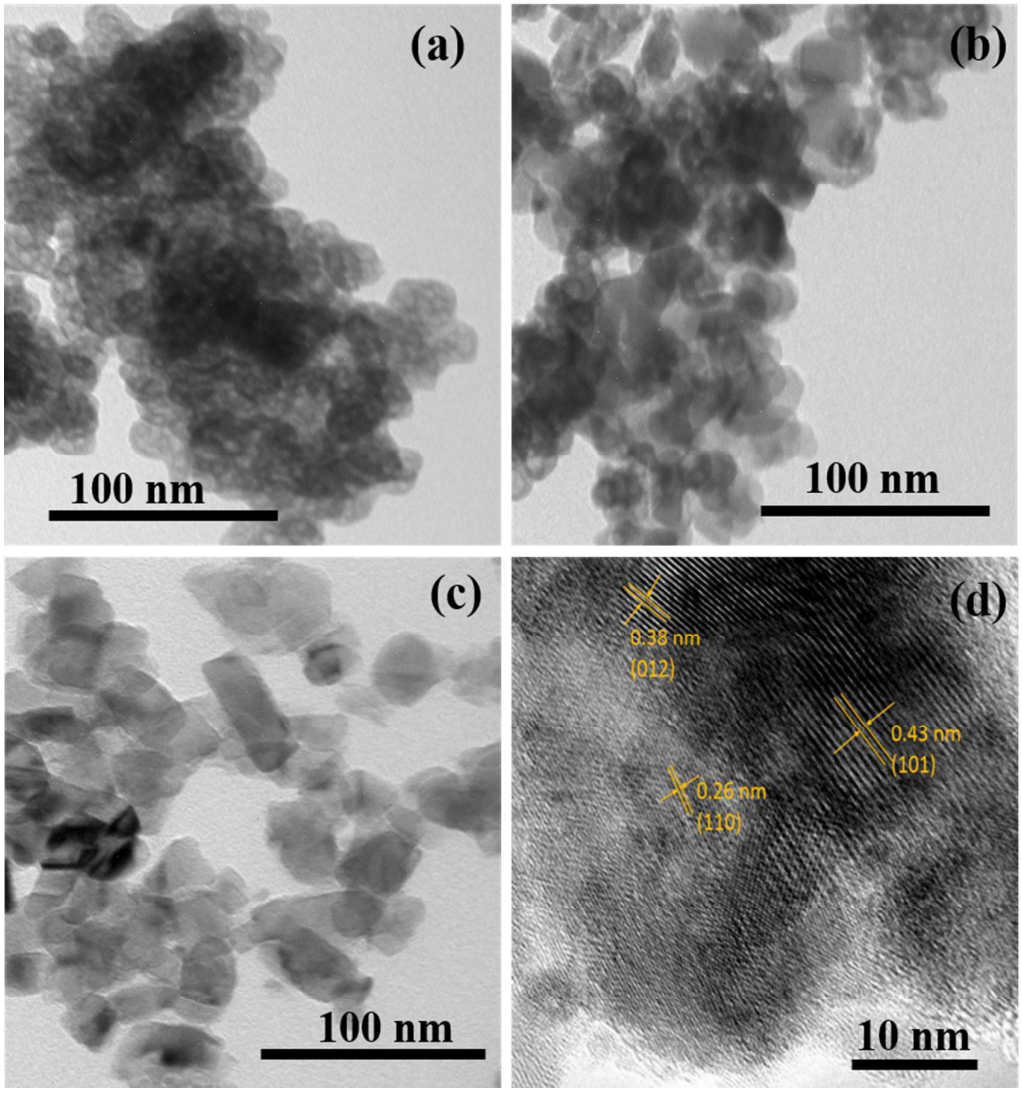

Fig. 2 TEM images of $CdTiO_3$ synthesized: (a) in absence of NaCl, (b) in presence of 0.075 M NaCl, (c) in presence of 0.25 M NaCl, and (d) HRTEM of $CdTiO_3$ synthesized in presence of 0.25 M NaCl.

The elemental composition was determined by the XPS. Fig. 3 shows the XPS spectra for $CdTiO_3$ synthesized in the presence of 1 mL 0.25 M NaCl. The full range of XPS spectrum for $CdTiO_3$ is depicted in Fig. 3a which shows peaks for Cl, C, Cd, Ti, and O. Fig. 3b shows the XPS spectrum of Cd 3d core levels. The binding energies at 3d 5/2 and 3d 3/2 are 405.1 eV and 411.8 eV, respectively, which correspond to Cd^{2+}.[30, 31] Fig. 3c represents the high resolution XPS spectrum for Ti where the binding energy at 2p 3/2=458.3 eV corresponds to Ti^{4+}.[32] XPS revealed that Cl^- is also present in $CdTiO_3$. Fig. 3d shows the XPS spectrum for Cl^- where binding energy at 2p 3/2=199.0 eV corresponds to Cl^-.[33] It is recently reported that Cl^- can be adsorbed on the surface of TiO_2 if it is present during synthesis.[34] Hence, it is assumed that in our experiments, Cl^- exists in the form of Cl^{-1} ions adsorbed on the surface of $CdTiO_3$. The full length XPS spectra for $CdTiO_3$ synthesized in the absence of NaCl and using 0.075 M NaCl are given in the supporting information (Fig. S4).

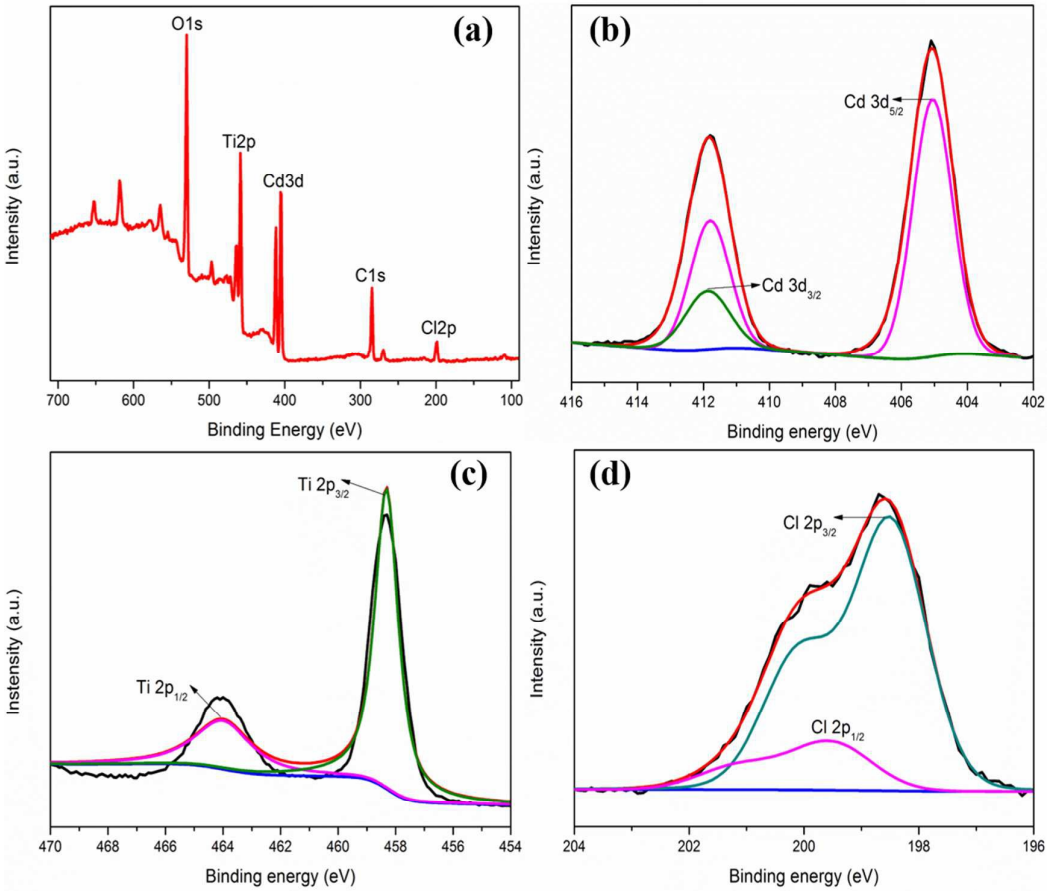

Fig. 3 XPS scans for $CdTiO_3$ synthesized in presence of NaCl: (a) survey of $CdTiO_3$, (b) Cd 3d scan, (c) Ti 2p scan, and (d) Cl 2p scan.

The optical properties of the as synthesized $CdTiO_3$ were evaluated by UV/vis spectroscopy. Fig. 4 shows the spectra for $CdTiO_3$ synthesized in presence and absence of NaCl. As it can be seen, there is no difference between the two spectra. Hence it is concluded that NaCl did not bring any change in the band gap and both types of $CdTiO_3$ would absorb same kind of light during irradiation. The band gaps of these samples have been determined by ploting $(Ahv)^{1/2}$ versus energy (hv)[35] and given in the supporting information (Fig. S5).

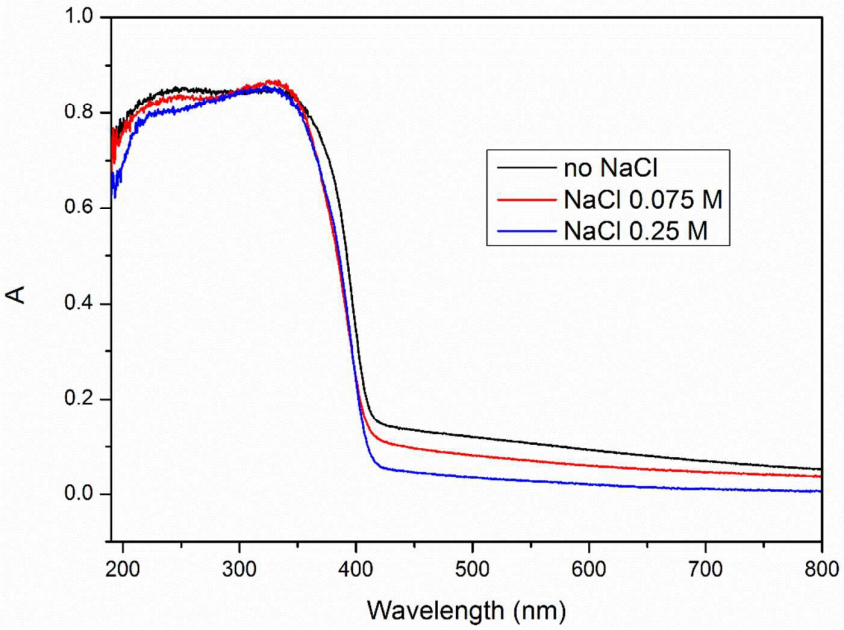

Fig. 4 UV/vis absorption spectra for $CdTiO_3$.

Photocatalytic degradation of methyl orange (MO) over $CdTiO_3$

The photocatalytic activity of $CdTiO_3$ was evaluated by degradation of MO under simulated sunlight. Prior to irradiation, the mixture of $CdTiO_3$ and aqueous solution of MO was stirred in dark for 30 min to achieve the adsorption equilibrium. After light irradiation, the MO solution began to decolorize. About 54% MO decolorization was achieved when the as synthesized TiO_2 was used as the photocatalyst. MO decolorization was very slow over the $CdTiO_3$ synthesized in the absence of NaCl. About 27% MO degradation (Fig. 5a) was achieved in 30 min light irradiation in this case. The photocatalytic activity was enhanced by a factor of more than two times when a slight amount of NaCl (1 mL, 0.075M) was added during the synthesis. It was found that the MO degradation was proportional to the amount of NaCl added during the synthesis. A degradation of 98% was achieved when 1 mL of 0.25 M NaCl was added. The MO solution became colorless within 25 min (Fig. S6) in this case. A

further increase in the NaCl concentration led to slightly less photodegradation of MO. The MO degradation decreased to 89% when NaCl concentration was further increased to 0.5 M during synthesis. This result indicates that an optimum amount of NaCl (1 mL of 0.25 M) is required to achieve the required crystallinity for the maximum photodegradation of MO under our experimental conditions. These results confirmed that the activity of $CdTiO_3$ towards MO photodegradation is directly proportional to the crystallinity which depends on the concentration of NaCl during synthesis.

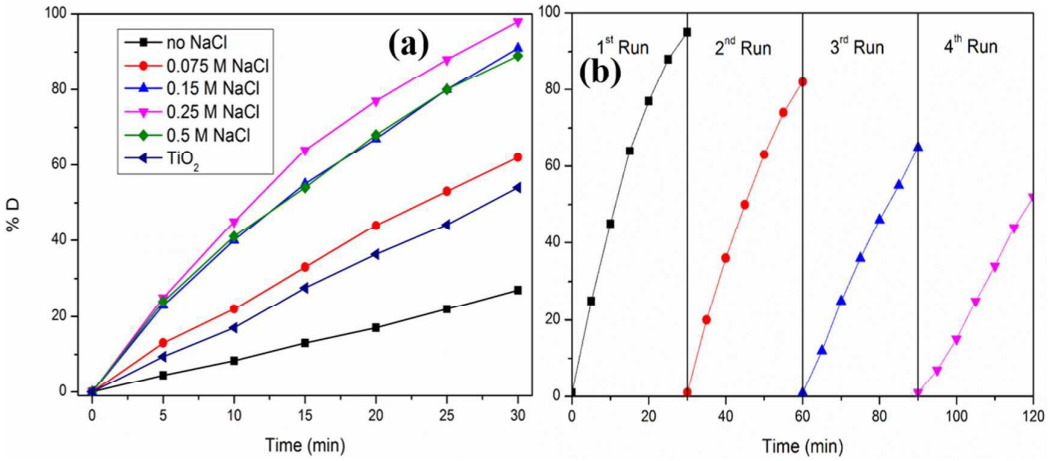

Fig. 5 (a) Effect of NaCl concentration during the $CdTiO_3$ synthesis on MO degradation under simulated sunlight and (b) recycling results.

The stability of the as synthesized photocatalyst was studied by recycling experiments. The as synthesized $CdTiO_3$ was found to be stable and active for four cycles as shown in Fig. 5b. The powder was separated by centrifugation and washed three times with deionized water after every run. A decrease in the activity was observed after every cycle which may be because of loss of the catalyst during centrifugation and washing.[36]

Surface area plays a very important part in determining the catalytic properties of a photocatalyst. In order to study the influence of chloride on the texture property of $CdTiO_3$, the N_2 adsorption/desorption isotherms were carried out at liquid nitrogen temperature after the samples were outgassed at 120°C. The specific surface area of the samples was calculated by using Brunauer-Emmett-Teller (BET) method. Pore size distribution and pore volume was determined by N_2 adsorption/desorption isotherms. The BET surface area of $CdTiO_3$ synthesized in the absence of NaCl was found to be 34.084 m^2/g while for the sample synthesized in the presence of 0.25 M NaCl, it was found to be 19.507 m^2/g (Table S1). The N_2 adsorption/desorption isotherms of the as synthesized $CdTiO_3$ samples are given in the supporting information (Fig. S7). This result indicates that the surface area actually decreased by increasing the amount of chloride during the synthesis. Hence, it is suggested that the surface area has no significant role for the photocatalytic activity of $CdTiO_3$ in our experiments.

The exact mechanism of how chloride can improve crystallinity is not clear at the moment. Chloride can be considered as an ionic ligand.[37] It is believed that when a ligand is adsorbed on the surface of a growing nanoparticle, the surface acts as a rigid barrier against the atomic rearrangement and Ligands are desorbed during heating which favors the particle crystallization.[22] Therefore, we suggest that during our experiments, chloride gets adsorbed on the surface of growing $CdTiO_3$. The adsorbed chloride gets desorbed during calcination due to which $CdTiO_3$ with increased crystallinity is obtained. Further studies on the role of ligands for higher crystallinity will improve our understanding of the underlying mechanisms.

$CdTiO_3$ with higher crystallinity showed highly enhanced photocatalytic activity. Improving crystallinity promotes the kinetics of charge diffusion.[15] The nanostructures with lower crystallinity have more defects which can act as recombination centers for photogenerated electrons and holes.[38] Highly crystalline materials can act as "a highway" for electrons, thus favoring better charge separation which results in enhanced photocatalytic activity.[7] Therefore, it is suggested that in our experiments, $CdTiO_3$ with higher crystallinity offered better charge separation which significantly enhanced the photodegradation of MO. On the other hand, $CdTiO_3$ with lower crystallinity presented more defects which significantly lowered the photodegradation of MO.

The suggested reason for enhanced photocatalytic activity was further confirmed by recording the PL spectra of the as prepared samples. PL measurements are applied to determine the charge separation behavior of the as synthesized samples.[39] Fig. 6 shows the PL spectra of the as synthesized samples measured with an excitation wavelength of 300 nm at room temperature. The PL spectrum of the sample prepared in the absence of NaCl shows a broad PL band signal which can be attributed to the radiative recombination of the excited species.[40] The PL emission for the sample prepared in the presence of 0.25 M NaCl is quenched which shows a better charge separation.

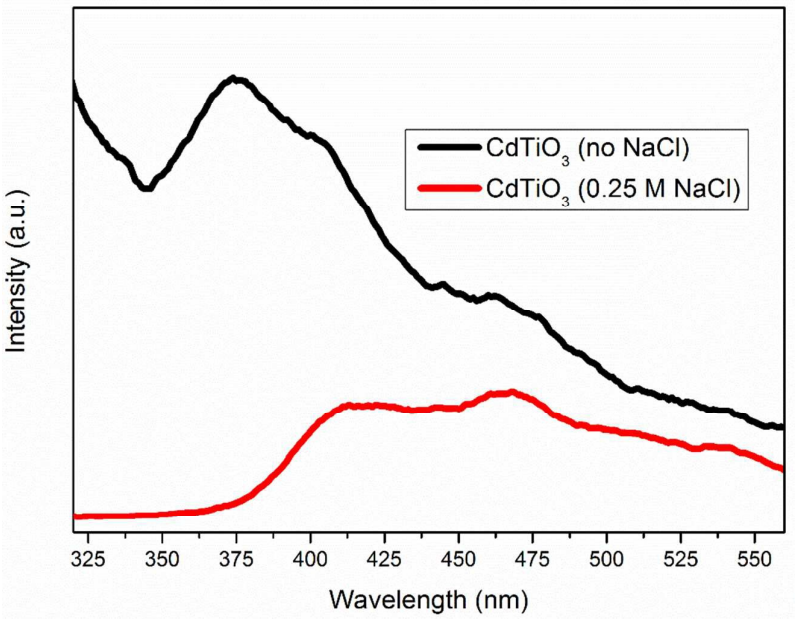

Fig. 6 PL spectra of as synthesized samples.

It will be worthy to mention that we also synthesized $CdTiO_3$ using $CdCl_2 \cdot 2.5H_2O$ as Cd precursor in the absence of NaCl. The obtained $CdTiO_3$ was compared with the $CdTiO_3$ synthesized from $Cd(NO_3)_2 \cdot 4H_2O$. Same trends were observed in the XRD patterns and the corresponding photocatalytic degradation of MO as found in the earlier experiments (Fig. S8). Hence it further confirmed that the higher crystallinity and photocatalytic activity was because of chloride ions present during the synthesis. The effect of bromide was also explored by introducing KBr instead of NaCl. However, Br was found ineffective to improve crystallinity or photocatalytic activity of $CdTiO_3$.

The mechanism of MO photodegradation over $CdTiO_3$ (synthesized using 0.25 M NaCl) under simulated sunlight was studied by applying scavengers. There are a number of active species responsible for the photodegradation of MO.[41] We used TEA as hole scavenger,[42] TBA as hydroxyl radical scavenger,[43] and *p*-BQ as superoxide

radical scavenger.[44] The scavengers were added to the photocatalytic mixture along with the $CdTiO_3$. As can be seen in Fig. 7, the photodegradation of MO was greatly inhibited in the presence of TEA (0.065 mL) and *p*-BQ (1 mg). These results indicate that the photogenerated holes and superoxide radicals played the major role in the photodegradation of MO during our experiments. Surprisingly, the MO degradation was slightly enhanced in the presence of TBA (1.25 mL). Such a trend for TBA has been observed by some other groups as well.[45, 46] This result shows that hydroxyl radical played a very little role in the MO degradation in our experiments. Secondly, it was suggested that the enhanced activity in the presence of TBA could be because of the formation of some unknown active species like $HO_2^{\bullet}$ or $^{\bullet}H$ which can contribute in photocatalysis.[45]

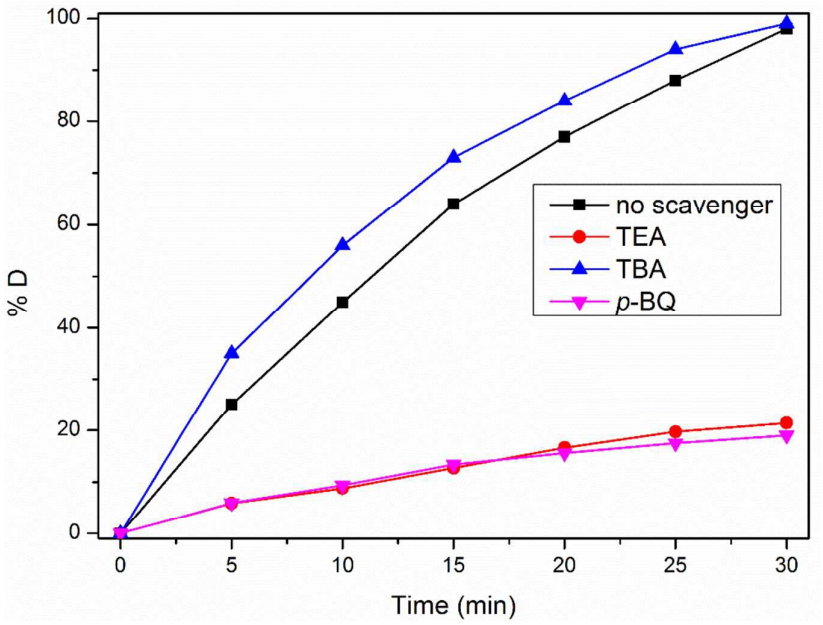

Fig. 7 Effect of scavengers on MO degradation over $CdTiO_3$.

The proposed mechanism for MO degradation over $CdTiO_3$ under simulated sunlight is shown in Fig. 8. Under simulated sunlight irradiation, the photogenerated

electron-hole pairs are formed. The photogenerated species recombine in the case of low crystalline $CdTiO_3$ while better charge separation is achieved in the case of highly crystalline $CdTiO_3$. The electrons are transferred to the conduction band (CB) while holes stay in the valence band (VB). The photogenerated electrons in the CB of $CdTiO_3$ can easily react with O_2 which results in the formation of superoxide radicals. The holes in the VB and newly formed superoxide radicals are highly active species which can readily degrade MO.

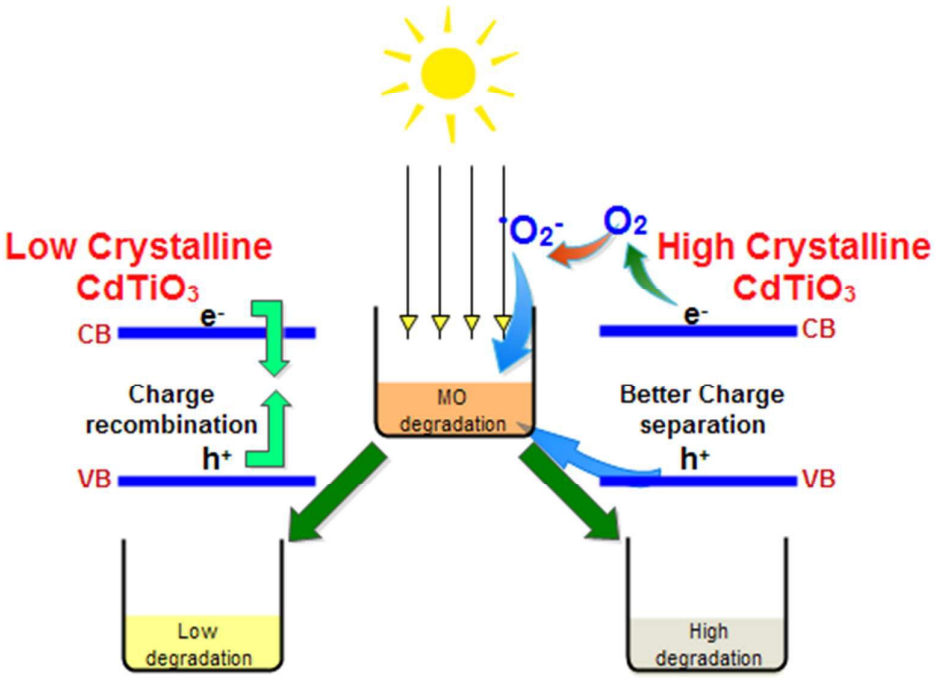

Fig. 8 Mechanism of MO photodegradation over $CdTiO_3$.

Conclusions

Highly crystalline $CdTiO_3$ was synthesized at mild reaction conditions in the presence of chloride which acts as a capping agent. $CdTiO_3$ with higher crystallinity showed highly enhanced photodegradation of MO. The photocatalyst was found to be stable and easy to separate. The concept of synthesizing highly crystalline semiconductor photocatalysts in the presence of a capping agent is worth exploring for other

photocatalytic materials. A combination of microemulsions and capping ligands for higher crystallinity may serve as a facile approach for the synthesis of highly active photocatalysts.

Supporting Information

Supporting information includes digital photographs captured during the synthesis, SEM images, EDS curves and elemental composition, XPS spectra, band gap plots, MO degradation patterns, and N_2 adsorption/desorption curves, BET surface area and pore volume for $CdTiO_3$ synthesized from $Cd(NO_3)_2 \cdot 4H_2O$; XRD patterns and photocatalytic activity of $CdTiO_3$ synthesized from $CdCl_2 \cdot 2.5H_2O$.

Acknowledgments

This work is supported by the Nationals Natural Science Foundation of China (Grants No. 21576044, 21536002 and 21176038, the Science Fund for Creative Research Groups of the National Natural Science Foundation of China (Grant No. 21421005), Dalian University of Technology Innovation Team (DUT2013TB07), and Shah ZH is thankful to Chinese Scholarship Council for financial support.

References

1. F. Amano, A. Yamakata, K. Nogami, M. Osawa and B. Ohtani, *J. Am. Chem. Soc.*, 2008, **130**, 17650-17651.
2. X. Chen, S. Shen, L. Guo and S. S. Mao, *Chem. Rev.*, 2010, **110**, 6503-6570.
3. W. Zhou, F. Sun, K. Pan, G. Tian, B. Jiang, Z. Ren, C. Tian and H. Fu, *Adv. Funct. Mater.*, 2011, **21**, 1922-1930.
4. A. Lannoy, R. Bleta, C. Machut, E. Monflier and A. Ponchel, *RSC Adv.*, 2014, **4**, 40061-40070.
5. G. Tian, H. Fu, L. Jing, B. Xin and K. Pan, *J. Phys. Chem. C*, 2008, **112**, 3083-3089.
6. K. Maeda and K. Domen, *J. Phys. Chem. Lett.*, 2010, **1**, 2655-2661.
7. T.-N. Ye, M. Xu, W. Fu, Y.-Y. Cai, X. Wei, K.-X. Wang, Y.-N. Zhao, X.-H. Li and J.-S. Chen, *Chem. Commun.*, 2014, **50**, 3021-3023.

8. J. Schneider, M. Matsuoka, M. Takeuchi, J. Zhang, Y. Horiuchi, M. Anpo and D. W. Bahnemann, *Chem. Rev.*, 2014, **114**, 9919-9986.
9. B. Liu, L. Ma, L.-C. Ning, C.-J. Zhang, G.-P. Han, C.-J. Pei, H. Zhao, S.-Z. Liu and H.-Q. Yang, *ACS Appl. Mater. Interfaces*, 2015, **7**, 6109-6117.
10. H. Kisch, *Angew. Chem., Int. Ed.*, 2013, **52**, 812-847.
11. J. Zhang, Q. Xu, Z. Feng, M. Li and C. Li, *Angew. Chem., Int. Ed.*, 2008, **47**, 1766-1769.
12. J. Zhang, M. Li, Z. Feng, J. Chen and C. Li, *J. Phys. Chem. B*, 2006, **110**, 927-935.
13. G. Liu, J. C. Yu, G. Q. Lu and H.-M. Cheng, *Chem. Commun.*, 2011, **47**, 6763-6783.
14. J. Pan, G. Liu, G. Q. Lu and H.-M. Cheng, *Angew. Chem., Int. Ed.*, 2011, **50**, 2133-2137.
15. X.-H. Li, J. Zhang, X. Chen, A. Fischer, A. Thomas, M. Antonietti and X. Wang, *Chem. Mater.*, 2011, **23**, 4344-4348.
16. X. Wang, L. Cao, D. Chen and R. A. Caruso, *ACS Appl. Mater. Interfaces*, 2013, **5**, 9421-9428.
17. V. N. Koparde and P. T. Cummings, *ACS Nano*, 2008, **2**, 1620-1624.
18. W. Tong, L. Li, W. Hu, T. Yan and G. Li, *J. Phys. Chem. C*, 2010, **114**, 1512-1519.
19. L. Li, J. Liu, Y. Su, G. Li, X. Chen, X. Qiu and T. Yan, *Nanotechnology*, 2009, **20**, 155706.
20. J. L. Yang, S. J. An, W. I. Park, G. C. Yi and W. Choi, *Adv. Mater.*, 2004, **16**, 1661-1664.
21. C.-H. Lu, W.-H. Wu and R. B. Kale, *J. Hazard. Mater.*, 2008, **154**, 649-654.
22. M. Epifani, E. Pellicer, J. Arbiol, N. Sergent, T. Pagnier and J. R. Morante, *Langmuir.*, 2008, **24**, 11182-11188.
23. B. Gilbert, F. Huang, Z. Lin, C. Goodell, H. Zhang and J. F. Banfield, *Nano lett.*, 2006, **6**, 605-610.
24. Y. Liu, C. Wang, Y. Wei, L. Zhu, D. Li, J. S. Jiang, N. M. Markovic, V. R. Stamenkovic and S. Sun, *Nano lett.*, 2011, **11**, 1614-1617.
25. K. Byrappa, N. Keerthiraj and S. M. Byrappa, in *Handbook of Crystal Growth (Second Edition)*, ed. P. Rudolph, Elsevier, Boston, 2015, pp. 535-575.
26. M. E. De Anda Reyes, G. Torres Delgado, R. Castanedo Pérez, J. Márquez Marín and O. Zelaya Ángel, *J. Photochem. Photobiol. A*, 2012, **228**, 22-27.
27. B. Pant, H. R. Pant, N. A. M. Barakat, M. Park, T.-H. Han, B. H. Lim and H.-Y. Kim, *Ceram. Int.*, 2014, **40**, 1553-1559.
28. M. R. Kim, K. Miszta, M. Povia, R. Brescia, S. Christodoulou, M. Prato, S. Marras and L. Manna, *ACS Nano*, 2012, **6**, 11088-11096.
29. M. R. Mohammadi and D. J. Fray, *Acta Mater.*, 2009, **57**, 1049-1059.
30. R. Islam and D. R. Rao, *J. Electron. Spectrosc.*, 1996, **81**, 69-77.
31. W. J. Danaher, L. E. Lyons, M. Marychurch and G. C. Morris, *Appl. Surf. Sci.*, 1986, **27**, 338-354.
32. D. Courcot, L. Gengembre, M. Guelton, Y. Barbaux and B. Grzybowska, *J.*

Chem. Soc. Faraday Trans., 1994, **90**, 895-898.
33. P. M. T. M. Van Attekum, J. W. A. Van der Velden and J. M. Trooster, *Inorg. Chem.*, 1980, **19**, 701-704.
34. L. Huang, R. Li, R. Chong, G. Liu, J. Han and C. Li, *Catal. Sci. Technol.*, 2014, **4**, 2913-2918.
35. C. Yu, G. Li, S. Kumar, K. Yang and R. Jin, *Adv. Mater.*, 2014, **26**, 892-898.
36. Z. H. Shah, J. Wang, Y. Ge, C. Wang, W. Mao, S. Zhang and R. Lu, *J. Mater. Chem. A*, 2015, **3**, 3568-3575.
37. C. Palencia, K. Lauwaet, L. de la Cueva, M. Acebron, J. J. Conde, M. Meyns, C. Klinke, J. M. Gallego, R. Otero and B. H. Juarez, *Nanoscale*, 2014, **6**, 6812-6818.
38. P. Tartaj, *Chem. Commun.*, 2011, **47**, 256-258.
39. C. Su, L. Liu, M. Zhang, Y. Zhang and C. Shao, *CrystEngComm*, 2012, **14**, 3989-3999.
40. J. Ng, S. Xu, X. Zhang, H. Y. Yang and D. D. Sun, *Adv. Funct. Mater.*, 2010, **20**, 4287-4294.
41. W. Li, D. Li, Y. Lin, P. Wang, W. Chen, X. Fu and Y. Shao, *J. Phys. Chem. C*, 2012, **116**, 3552-3560.
42. A. Reynal, F. Lakadamyali, M. A. Gross, E. Reisner and J. R. Durrant, *Energy. Environ. Sci.*, 2013, **6**, 3291-3300.
43. Y. Zhu, Y. Wang, W. Yao, R. Zong and Y. Zhu, *RSC Adv.*, 2015, **5**, 29201-29208.
44. D. Wang, L. Guo, Y. Zhen, L. Yue, G. Xue and F. Fu, *J. Mat. Chem. A*, 2014, **2**, 11716-11727.
45. T. Yan, R. Yuan, W. Li and J. You, *Appl. Catal. A-Gen.*, 2014, **478**, 204-210.
46. W. Li, D. Li, J. Xian, W. Chen, Y. Hu, Y. Shao and X. Fu, *J. Phys. Chem. C*, 2010, **114**, 21482-21492.